Hindawi
Geofluids
Volume 2023, Article ID 6187764, 11 pages
https://doi.org/10.1155/2023/6187764

Research Article

Optimization of Carbon Dioxide Foam Fracturing Technology for Shale Gas Reservoir

Chaoli Gao,[1,2] Shiqing Cheng,[1] Mingwei Wang,[3] Wen Wu,[4] Zhendong Gao,[5] Song Li,[6] and Xuangang Meng[5]

[1]*State Key Laboratory of Petroleum Resources and Prospecting, China University of Petroleum, Beijing 102249, China*
[2]*Exploration and Development Technology Research Institute, Yanchang Oil Field Co., Ltd., Yanan 716000, China*
[3]*School of Oil & Natural Gas Engineering, Southwest Petroleum University, Chengdu 610500, China*
[4]*PetroChina Southwest Oil and Gas Field Company, Chengdu 610041, China*
[5]*Technology and Information Management Department of Yanchang Oilfield Co., Ltd., Yanan 716000, China*
[6]*Engineering Research Institute of PetroChina Southwest Oil and Gas Field Company, Chengdu 610017, China*

Correspondence should be addressed to Shiqing Cheng; chengsq973@163.com

Received 22 August 2022; Revised 19 October 2022; Accepted 18 January 2023; Published 13 February 2023

Academic Editor: Peng Tan

Major shale gas exploration and development fields are located in the Sichuan basin. It requires huge water sources for shale gas fracking, but the well sites are mostly in the hills, which limits the industrialization of shale gas development. CO_2 foam fluids can meet the requirements of fracking fluids and relieve water stress. It analyzed the feasibility of CO_2 foaming fracturing for shale gas formation fracturing, proposed a design philosophy for CO_2 foaming fracturing, and optimized fracturing parameters such as foam mass, proppant concentration, friction, and discharge rate. The flowchart of CO_2 foam fracturing was established in, where the fracture morphology and propagation behavior of CO_2 foam fracturing were obtained from numerical simulations comparable to the hydraulic fracture generated by conventional hydraulic fracturing. The CO_2 foaming fracturing technique can provide a discharge rate of 6.0 m^3/min and fluid volume and captures the volume effect of the current stimulated reservoir, which needs to be improved. It can be considered an initial survey of CO_2 foam fracturing available in the Sichuan Basin shale formation, which may provide new methods and clues for stimulation.

1. Introduction

Shale gas reserves are abundant in China. It is predicted that shale gas geological reserves in China are 134.42 trillion square meters and the recoverable resource potential is 25.08 trillion square meters, which is roughly equivalent to the 28 trillion squares of technology available in the United States [1, 2]. According to the development experience of the United States, the slick water volume fracturing technology of horizontal well is the key core technology for efficient development of shale gas reservoirs, but this fracturing technology needs to consume a lot of water, and the most favorable areas for shale gas exploration and development in China are located in or adjacent to areas with long-term or seasonal water shortage. Clay mineral content is relatively abundant in domestic shale gas reservoirs, particularly in domestic continental shale gas reservoirs. The mineral content of the clay is even greater than 60%. When traditional water-based fracturing fluids invade shale reservoirs, clay minerals expand with water and cause great permeability damage to shale reservoirs [3–7]. In addition, domestic shale gas formations are generally low in pressure. When conventional water-based fracturing fluids are used for shale gas development, water consumption is excessive, reservoir damage is severe, and return rates are low. Therefore, for developing shale gas reservoirs in China, it is impossible to just copy foreign technology, and an advanced fracturing technology with minor water consumption (or even no

water), no pollution to the environment, and minor damage to the reservoir is needed.

In order to overcome the shortcomings of conventional fracturing technology, researchers began to study foam fracturing technology in the 1970s [8]. Since the first completion of foam fracturing in Lincoln County, West Virginia, foam fracturing technology has evolved from the original N_2 foam fracturing to the current CO_2 foam fracturing. In 1986, a 60% CO_2 foam fracturing fluid was used to fracture the carboniferous gas reservoir at Fez Dolf [9]. The buried depth of the gas reservoir was 3400-3650 meters underground. After fracturing, the natural gas production has increased by approximately 12 times [10]. By the 1990s, about 90% of gas wells and 30% of oil wells in the United States and Canada had adopted CO_2 foam fracturing technology [11].

Emrani et al. [12, 13] believed that foam is a two-phase system consisting of liquid, compressible gas, and chemicals (surfactant or polymer) to enhance fluid stability or viscosity, and the trend of decreasing surface area leads to foam degradation into separated gas and liquid phases. The CO_2 foam fracturing fluid has the advantages of strong sand pack ability, high viscosity, minimal water consumption, minor reservoir damage, etc. and has achieved significant production increasing in low-pressure and low-permeability water-sensitive sandstone, coalbed methane, and shale gas reservoir reconstruction [13–22].

Liquid CO_2 can also be a good option for restoring flow channels in wells with severe near borehole damage, or in reservoirs with undesirable long fractures. Mazza [23] believes that liquid CO_2 is most suitable for low-pressure and dry gas reservoir stimulation, because the previous fracturing fluid will destroy gas permeability. Xiao et al. [24] and Wang et al. [25] believe that foam has been widely used in unconventional reservoir fracturing, and it has more advantages than water-based fracturing fluid, such as less water consumption, rapid flowback, low filtration, and high sand carrying. Due to the significant temperature difference between the reservoir rock and the pumped fracturing fluid, the reservoir rock will be cooled. Alqatahni et al. [26] believed that the cooling effect of fracturing fluid may destroy the cementation in rock particles and change the pore structure. Grundmann et al. [27] pointed out that when the liquid nitrogen is heated to the reservoir temperature, the liquid CO_2/N_2 is converted to the gas state, causing its flow rate to increase by about eight times, which is helpful to carry the proppant to the deeper position of the reservoir. It is thought that extreme temperatures cause rock to contract and water to expand, creating local stress differences that cause cracks. Due to the inhomogeneous distribution of thermal stress, numerous microscopic fractures can appear in the interior and on the surface of the rock [28]. Fu and Liu [29] believed that the anhydrous fracturing technology is the key to effectively improve the recovery of unconventional resources and also solved the problems of reducing water consumption and environmental pollution. They developed two main anhydrous fracturing fluids (foam and liquid CO_2/N_2) and introduced the advantages and challenges of anhydrous fracturing, fracturing mechanism, and fluid properties (such as stability and rheology). Shen et al. [30] developed a clean high-temperature-resistant CO_2 foam fracturing fluid suitable for shale reservoir fracturing, which significantly affects the field trial of the Yanchang oilfield and the effect of increasing production is significant.

Tan et al. [31] completed a large-scale true triaxial sand fracturing experiment using the deep Longmaxi shale outcrop in Sichuan Basin, China, studied the hydraulic fracture (HF) propagation and proppant migration mechanism, and discussed the interaction between vertical HF and bedding plane (BP). They also used the extended finite element method (XFEM) based on the viscous zone model (CZM) to establish a numerical model of transversely isotropic layered shale with a transition zone and clarified the influence of fracturing parameters on the longitudinal propagation behavior of fracturing fractures [32]. Fu and Liu simulated and studied the rheology and stability of CO_2 foam under high-temperature and high-pressure experimental conditions [33]. Wang et al. [34] optimized the formula of CO_2 gel fracturing fluid for shale gas reservoir with experiments and studied the rheological characteristics of CO_2 foam gel fracturing fluid with different CO_2 foam qualities under two conditions of high temperature (65°C) and high pressure (30 MPa), as well as nonfoaming and foaming through indoor pipe flow. Cai et al. [35] studied the fracture initiation and extension behavior during supercritical carbon dioxide injection fracturing, established an induced strain model, and systematically studied the influencing factors of fracture initiation.

The feasibility of CO_2 foam fracturing for shale gas reservoirs was analyzed in this paper. The application of CO_2 foam fracturing techniques to shale gas reservoirs was discussed, and the designing parameters for CO_2 foam fracturing, fracture morphology, and spreading behavior were studied. The aim is to provide fresh ideas and methods for shale gas stimulation.

2. Simulation of CO_2 Foam Fracturing Design

2.1. Ideas for Foam Fracturing Design. Given the current research results and field construction experience of CO_2 foam fracturing in China [36], combined with the goals and ideas of shale reservoir fracturing in the Sichuan Basin, the following ideas are proposed for CO_2 foam fracturing design:

(1) Foam quality of CO_2 foam fracturing fluid: the foam quality of CO_2 foam should be selected according to the characteristics of the reservoir, taking into account the geometrical dimensions of the fracture, reducing the secondary damage to the reservoir during the fracturing process, and improving the fracture conductivity and other geological and engineering factors and the principle of economic benefits of input and multioutput. No one-sided pursuit of high foam quality and increased construction size are advocated

(2) CO_2 foam pump injection volume: the determination of CO_2 foam pump injection volume needs to

take into account factors such as tube friction, sand carrying performance, and foam quality

(3) CO_2 foam fracturing design model: among the currently used fracturing software, FracPro 2012 is a software that is widely used in fracturing optimization design that includes a CO_2 foam fracturing design module. Quasi-3D fracturing models were used to calculate the temperature profile of the borehole, fracture, and CO_2 foam mass

2.2. Key Parameters of the CO_2 Foam Fracturing Design

2.2.1. Foam Quality. The CO_2 foam mass is the ratio of the gaseous CO_2 to the total foam fracturing fluid at a certain temperature and pressure. In general, CO_2 foam fracturing refers to foam mass greater than 52% to 70%, and when the foam mass reaches 100%, it is called dry CO_2 fracturing. The foam mass of CO_2 foam is a function of temperature and pressure. The gas volume obeys the equation of the state of a real gas:

$$V_g = \frac{\mathrm{nZRT}}{P}. \tag{1}$$

When the gas turns from state 1 to state 2,

$$\frac{V}{V_{g1}} = \frac{Z_2 T_2 P_1}{Z_1 T_1 P_2}. \tag{2}$$

Let the liquid volume be V_1, which is defined by the definition of foam quality:

$$V_1 = V_g\left(\frac{1}{\Gamma - 1}\right). \tag{3}$$

Since the liquid is approximately incompressible, when the gas state changes, the mass of pure foam fluid is calculated as

$$\frac{1}{\Gamma_2} = \frac{(1-\Gamma_1)Z_1 T_1 P_2}{\Gamma_1 Z_2 T_2 P_1} + 1. \tag{4}$$

When the foam fracturing fluid carries sand, the proppant is uniformly distributed in the foam, which is a discontinuous phase. This property can be thought of as the internal phase of the fracturing fluid, with the liquid being the external phase [37]. The foam mass of a foam fluid with a proppant is calculated as follows:

$$\begin{aligned} \Gamma_s &= \frac{V_I}{(V_I + V_O)} = \Gamma + (1-\Gamma)C_{sf}, \\ \Gamma_s &= \frac{V_I}{(V_I + V_O)} = \Gamma + (1-\Gamma)C_{sf}. \end{aligned} \tag{5}$$

For constant foam quality design, the design of a fracture construction program in which constant jellium and liquid CO_2 displacements are injected into the well to maintain foam quality, as is shown in Figure 1. The advantage is that it is easy to construct and control. The downside is that it is hard to take advantage of foam fracturing. For scope of application, this is mainly used for fracturing construction with low foam quality (CO_2 is accompanied by fracturing). For variable foam quality design, according to the fracturing construction program, the discharge of jelly liquid is from minor to large, liquid CO_2 displacement is injected into the well from large to minor, and foam quality is continuous or phased (commonly from high to low). Pros are as follows: taking full advantage of the foam's low fluid loss and low damage, as well as improved salability. Cons are as follows: It is more difficult to refine fracking sand, and the construction process was more involved. Construction control is also difficult. Application includes water sensitivity, water lock damage formation, and construction to determine foam fracture.

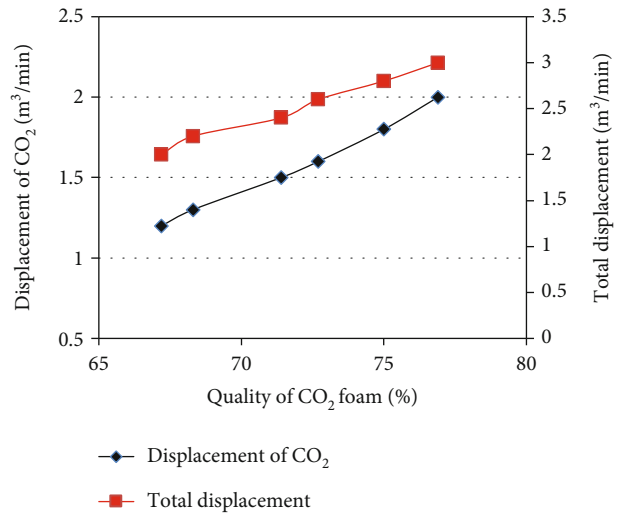

Figure 1: Pump rate and CO_2 foam quality of variable quality.

In constant internal phase, external phase design, phase here refers to the three phases of gas, liquid, and solid in a fracturing fluid. In the fracturing design, the design of the relevant parameters and process for incorporating the proppant (solid phase) into the CO_2 (gas phase) is called constant internal phase design (Figure 2). The converse is a constant external phase design. Liquid CO_2 has been converted into gas in the formation. When calculating the foam mass, the volume of the liquid CO_2 foam is calculated according to the gas state formula. The volume of liquid CO_2 converted to a gaseous state can be calculated from the formula for the nonideal gas state by counting only its compression coefficient.

2.2.2. CO_2 Foam Quality and Sand Ratio Simulation. Most fracturing fluids are non-Newtonian fluids. Fractured fluids are often treated as power-law fluids in theoretical studies and engineering calculations. The power-law model formulation calculates the apparent viscosity of the fracturing fluid [38].

$$\eta = \frac{\tau}{\gamma} = K\gamma^{n-1}. \tag{6}$$

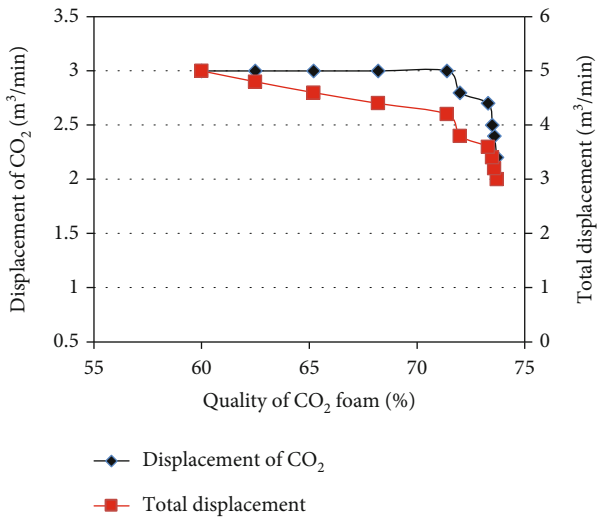

FIGURE 2: Pump rate and CO_2 foam quality of constant internal term.

The shear rate at which a property settles in a fracturing fluid is defined as

$$\gamma_P = \frac{3v_t}{d_p}. \tag{7}$$

The apparent viscosity can be calculated by substituting formula (6) into formula (7).

$$\eta = K\gamma_p^{n-1} = \left(\frac{3v_t}{d_p}\right)^{n-1}. \tag{8}$$

The Reynolds number of proppant particles in fracturing fluid can be calculated by substituting formula (8) into formula (7).

$$N'_{\mathrm{Re}} = \frac{d_p^n 3v_t^{2-n} P_f}{3^{n-1}K}. \tag{9}$$

Substituting formulas (6) and (8) into formula (9), the settling velocity of proppant particles in the laminar flow region of the power-law fluid can be obtained [39].

$$v_t = \left[\frac{gd_p^{n+1}\left(P_{P\_}P_f\right)}{18K3^{n-1}}\right]^{1/n} \quad N'_{\mathrm{Re}} \le 1. \tag{10}$$

The above formulas are the calculation formulas of the settlement velocity of a single particle in a power-law fluid under ideal conditions. There are certain deviations in practical application. Dazhi and Tanner [40] used a numerical simulation method for spherical particles in the power law. The settlement formula in the fluid is corrected, and the correction coefficient α for the resistance coefficient is obtained. Experimental results show that the grain-to-sand ratio has a large effect on the settling velocity, so the effect of the grain-to-sand ratio must be taken into account when analyzing the settling velocity. The formula commonly used to describe the effect of sand ratio on settling velocity is as follows: $u_{\mathrm{to}}/u_{ts} = 1 + AC_S$ or $u_{\mathrm{to}}/u_{ts} = (1 - C_S)^m$. The former formula applies to the case where the sand ratio is less than 5%. Because the sand ratio range is more than 5% in this experiment, Therefore, using the form $u_{\mathrm{to}}/u_{ts} = (1 - C_S)^m$ to fit the computational correlation, the function form of the computational correlation can be obtained as

$$u_{t=d_s}\left[\frac{gd_s(P_{s\_}P_l)}{18K'\left(A + Bn' + Cn'^2\right)}\right]^{1/n}(1 - C_S)^m. \tag{11}$$

Based on formula (11), the above experimental results are analyzed and processed, and the influence of sand ratio, temperature, and foam quality on the settlement speed is considered; the publicity is modified and fitted, as shown in formula (12). Calculation of particle settling velocity correlation is as follows:

$$u_{t=d_s}\left[\frac{gd_s(P_{s\_}P_l)}{18K'(0.801 - 1.24n + 9.973n^2)}\right]^{1/n}(1 - C_S)^{0.9896}. \tag{12}$$

The diameter of the spherical particle is replaced by the equivalent diameter of the particle, which takes the value $d_s = 0.5$ mm. The density of the proppant particles is about 1700 kg/m^3. Figure 3 is a comparison of the calculated and final measured values of the final settling velocity at the time of foaming, with an associated average error of 13.2%. The scope of application of this formula is as follows: $0 \le C_S \le 10\%$, $45\% \le \Gamma \le 75\%$, $35 \circ C \le T \le 80 \circ C$, and $P = 10$ MPa.

2.2.3. Friction and Pressure Simulation. In the case of the quantitative transfer of the momentum transfer between the fluid phases, the frictional force at the phase interface, and the shear rate cannot be quantitatively described. Therefore, the effect of various physical and dynamical parameters in the system on the friction drag coefficient can be expressed by the following formula:

$$\lambda = f(P, T, \rho, u, D.L). \tag{13}$$

The dimensionless effect of each factor is available:

$$\lambda = f\left(\mathrm{Re}'\right). \tag{14}$$

The calculation of the turbulent smooth zone of non-Newtonian fluids can also be combined with the Newtonian fluid by expanding the generalized Reynolds number. The coefficient of resistance λ for the smooth region of the tube flow depends not only on the generalized Reynolds number Re' but also on n'. There are usually two calculation methods.

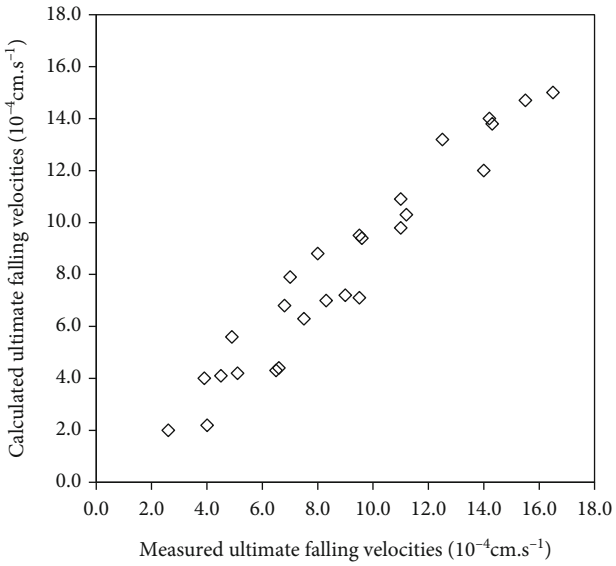

Figure 3: Comparison of the simulated and measured ultimate falling velocities.

(1) Brassian-Type Empirical Formula.

$$\lambda = \frac{a}{\mathrm{Re}'^{b}}, \tag{15}$$

where a and b are functions of the flow index n', and a and corresponding to different n' values can be derived in the form of data fitting.

(2) Semiempirical Formula. A semiempirical formula for calculating the drag coefficient λ of a non-Newtonian fluid turbulent smooth zone according to the Karman formula:

$$\frac{1}{\sqrt{\lambda/4}} = \frac{4}{n'^{0.75}} \lg \log_{10}\left[\mathrm{Re}'\frac{\lambda}{4}^{\left(1-\left(n'/2\right)\right)}\right] - \frac{4}{n'^{0.5}}. \tag{16}$$

The theoretical calculations of formula (9) are consistent with the experimental data. The experimental data range is $n' = 0.36 \sim 1.00$, $\mathrm{Re}' = 2900 \sim 3600$.

In this study, the fitting form of the first empirical formula was selected, and the mathematical model of the friction coefficient of CO_2 foam fracturing fluid was established. The correlation between the frictional resistance coefficient of CO_2 foam fracturing fluid and the generalized Reynolds number is obtained:

(1) In the case of no foaming:

$$\lambda = 50.917\mathrm{Re}'^{-0.95255} \tag{17}$$

Figure 4(a) shows the fit of the friction coefficient to the generalized Reynolds number. The correlation coefficient is 0.9983. The average margin of error is 1.10%. The scope of application of this formula is $85 \le \mathrm{Re}' \le 2004$, $45\% \le \Gamma_{TH} \le 75\%$, $0 \circ C \le t \le 30 \circ C$, and $10\,\mathrm{MPa} \le P \le 40\,\mathrm{MPa}$.

(2) In the case of foaming:

$$\lambda = 91.436\mathrm{Re}'^{-1.07175} \tag{18}$$

Figure 4(b) shows the fit of the friction drag coefficient to the generalized Reynolds number. The correlation coefficient was 0.9991 with an average error of 5.73%. The scope of application of this formula is $74 \le \mathrm{Re}' \le 1142$, $45\% \le \Gamma \le 75\%$, $35 \circ \mathrm{C} \le t \le 80 \circ C$, and $10\,\mathrm{MPa} \le P \le 40\,\mathrm{MPa}$.

According to the above two formulas, the friction of the CO_2 foam fracturing fluid under laminar flow conditions can be predicted. Indoor pipe friction tests are limited to friction tests in laminar flow conditions due to the limitations of the experimental pipe and pump flow. In actual fracking construction, the flow of fracked fluid in the pipe is mostly turbulent [41]. For the frictional drag of CO_2 foam fracturing fluid in a tube under turbulent flow conditions, this study predicts the frictional coefficient under turbulent flow conditions based on the results of rheological tests in laminar flow conditions combined with the Kemblowsk-Kolodziejsk equation:

$$\lambda = 0.002225e^{\left(\exp\left(0.572\left(\left(1-n^{4.2}\right)/n^{0.435}\right)1-n^{4.2}/n^{0.435}\right)^{1000/\mathrm{Re}'}\right)/\mathrm{Re}'^{\left(0.314n^{2.3}-0.064\right)}},$$
$$\mathrm{Re}' = \frac{\rho V D}{k}\left(\frac{4n}{3n+1}\right)^{n}\left(\frac{8V}{D}\right)^{(1-n)}, \tag{19}$$

where λ is the friction coefficient, n is the flow index, k is the consistency coefficient, Re' is the generalized Reynolds number, V is the flow rate (m/min), and D is the pipe diameter (m).

When $\mathrm{Re}' > 31600/n^{0.435}$, calculated using the following:

$$\lambda = \frac{0.0791}{\mathrm{Re}'^{0.25}}. \tag{20}$$

When predicting turbulent friction, first determine the value of the flow index and consistency coefficient according to working conditions, calculate the generalized Reynolds number by substituting the equation, then calculate the friction coefficient, and finally calculate the pressure drop according to the Darcy equation.

2.2.4. Construction Displacement. The construction displacement is a key parameter in fracture design, which will affect the pumping pressure and fracture geometry. The construction displacement mainly depends on factors such as fracture injection mode, fracture column, wellhead pressure, and fracture equipment power. The height of the break has some influence. The displacement in the construction of liquid CO_2 foam fracturing depends primarily on the number of liquid CO_2 storage tanks at the well site. Since liquid

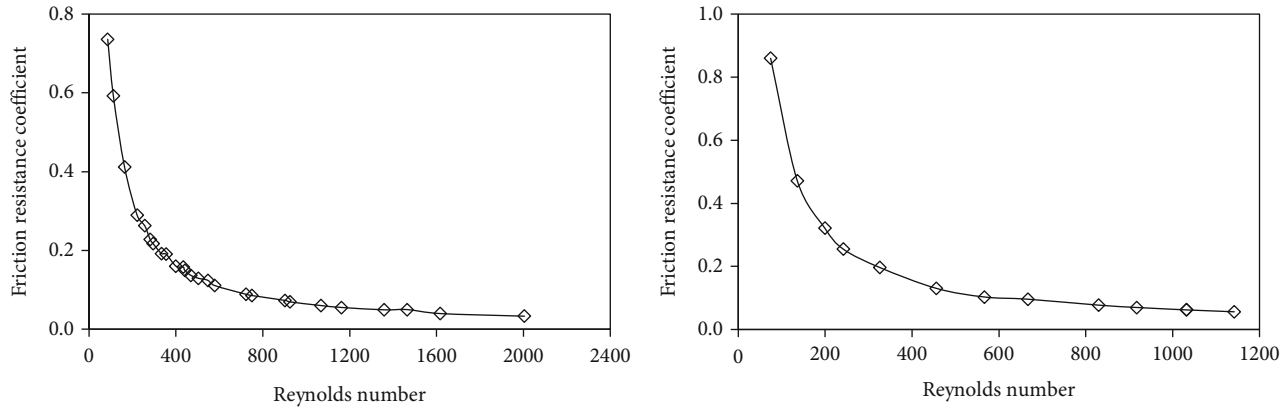

(a) Condition of unbubbly

(b) Condition of bubbly

Figure 4: Matching relationship between the frictional factor and generalized Reynolds number.

Table 1: Relationship of CO_2 foam rates on condition of ground surface and downhole.

CO_2 foam rates on the condition of the ground surface (m^3/min)	CO_2 foam rates on condition of downhole (m^3/min)
1.00	1.31
1.50	1.96
2.00	2.62
2.50	3.27
3.00	3.93
3.50	4.58
4.00	5.23
4.50	5.89
5.00	6.54

CO_2 storage tanks are not like regular acid storage tanks, the construction displacement is limited.

After a certain pumping displacement of the ground, a mixture of fracturing fluid and liquid CO_2 enters the formation. Due to changes in the working environment such as pressure and temperature, liquid CO_2 begins to vaporize and form foam, and the volume of the mixed fluid increases. A certain amount of mixed fluid, consisting of ground fracturing fluid and liquid CO_2, will expand in volume in the formation environment, which is equivalent to an increase in the bottom hole displacement. The equivalent bottom hole foam fluid displacement is calculated as follows:

(1) The pressure of pumping CO_2 from the ground is 35 MPa, the temperature is 18°C, and the density ρ_1 is 1060 kg/m^3. If the displacement Q_1 is 1.0 m^3/min, the mass per unit time passing through the cross-sectional area of the tubing is $Q = Q_1 \blacksquare \rho_1 = 1050 \times 1.0 = 1050$ kg/min

(2) When CO_2 enters the reservoir, the temperature increases and the volume expands. From the reservoir conditions (temperature: 43.6°C, pressure: 22.23 MPa), the density ρ_2 of CO_2 is 810 kg/m^3, according to the conservation of CO_2 mass, the CO_2 displacement Q_2 under reservoir conditions is $Q_2 = Q/\rho_2 = 1060/810 = 1.309$ m^3/min

(3) Under the condition of wellhead and reservoir conditions, the density difference is small, that is, the expansion is small, and it can be approximated that the displacement under the wellhead condition and the reservoir condition is still equal: $Q_{\text{Base liquid}} = 1.0$ m^3/min

(4) Therefore, the foam quality of CO_2 foam fracturing fluid under reservoir conditions is as follows: $\Gamma = V_{CO_2}/(V_{CO_2} + V_{\text{Base liquid}}) = 1.309/(1.309 + 1.0) = 56.7\%$

The equivalent bottom hole CO_2 foam fracturing fluid displacement is $Q_{\text{Equivalent}} = Q_2 + Q_{\text{Base liquid}}$.

According to the above method, the equivalent CO_2 foam displacement at the bottom of the well can be calculated, as shown in Table 1.

According to the test results of the rheological properties of the CO_2 foam fracturing fluid, before the liquid CO_2 is not vaporized, the CO_2 has a "dilution" effect on the pure fracturing fluid, and the viscosity is lowered. To avoid the sedimentation of the proppant in the sand-crushing fluid entering the wellbore and near-well zone, the pumping displacement of the cleaning fracturing fluid should not be lower than 1.0 m^3/min; the viscosity of the CO_2 foam fracturing fluid system is lower, to improve its carrying sand capacity, and total pumping displacement of fracturing fluid and liquid CO_2 should not be lower than 2.0 m^3/min. According to the injection method, the structure of the fracturing column, and the scale of the fracturing, the total construction displacement is 2.5 ~ 5.0 m^3/min.

2.2.5. Preliquid Ratio. According to the "bubble quality" design idea, the pumping ratio (foam quality) of liquid CO_2 in the preliquid phase is higher than that in the sand-carrying stage. Taking this into account, the fraction of pre-fluid foam fracturing is 25.0% to 35.0%.

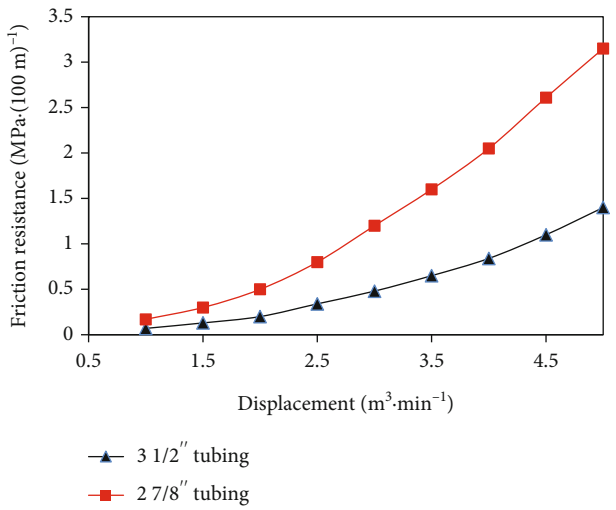

Figure 5: The relationship between pump rate and friction of CO_2 foamed fracturing (60%).

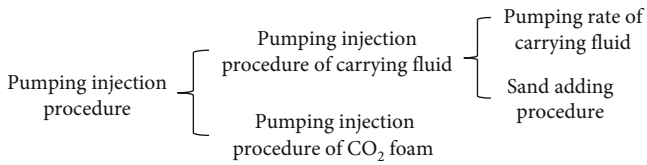

Figure 6: The pumping process of carbon dioxide foam fracturing.

2.2.6. Proppant Concentration (Sand Ratio). In order to obtain an optimized fracture design, the efficiency of the stimulation and conversion of the gas well is optimized, and the optimized fracture length and conductivity are obtained based on the characteristics of the reservoir and its production capacity. However, parameters such as scale, prefluid volume, displacement, and sand concentration in the fracture design are strongly sensitive to the seam length and fracture conductivity, with sand concentration being the most sensitive to conductivity. Whether the sand concentration is reasonable will directly affect the effectiveness and long-term and economic impact of fracking measures.

(1) Sand concentration optimization principle

The formula for calculating the dimensionless conductivity in the fracturing design is as follows:

$$F_{cd} = \frac{k_f w_f}{kL_f}(1 - D), \tag{21}$$

where k_f is the fracture permeability, mD; w_f is the average fracture width closed on proppant, mm; k is the reservoir permeability, mD; L_f is the fracture half-length, m; and D is the fracture permeability damage coefficient.

There are many influencing factors involved in the formula. Three key uncertain parameters of many factors directly affect the final yield increase effect, which are the dimensionless conductivity F_{cd}, the fractured support joint length x_f, and the guiding ability K_{wf} provided by the support fracture.

(2) Sand concentration optimization method

(a) Optimization of fracture support length

The determination of a reasonable support fracture length is mainly determined by empirical methods and economic optimization. There are many uncertainties in the production capacity prediction results. Elkins proposed the optimal slit length partitioning reference standard for different permeability conditions without considering other factors. When using the fracture length criterion proposed by Elkins et al. [36], it must be combined with reservoir-specific characteristics and single-well scale optimization results.

(b) Optimized design of sand pumping program

The ground sanding procedure is directly related to the geometrical size of the sand-filled fracture and its conductivity distribution, which is also a fundamental factor affecting the fracturing effect. Nolte's liquid efficiency linear-sloped ground sanding pump injection procedure is the theoretical basis for obtaining an ideal sanding profile within a fracture.

(c) Sand concentration optimization steps

The sand concentration optimization step consists of determining the optimal fracture length x_f and scale, based on the reference value of the fracture length required by Elkins for different permeabilities, combined with the reservoir permeability K, and the block optimization results. According to the formula, F_{cd} and reservoir permeability K and the optimal fracture length x_f calculate the actual fracture conductivity $(Kw)_f$, or the remaining conductivity in the fracture. Based on the reservoir parameters of the target layer and the size of the fracture construction, see the linear slope proposed by Nolte et al. [42]. The optimal sanding pumping procedure is designed for sanding to obtain the average ground sanding proppant concentration at the desired fracture conductivity.

Based on the results of tests on the dynamic sand-carrying performance of CO_2 foam fracturing fluid, the viscosity of CO_2 foam fracturing fluid is lower, but the sand-carrying capacity is comparable to that of acid crosslinked silicone foam fracturing fluid. For CO_2 foam fracturing in shale gas reservoirs, a sand ratio of 18.0% to 22.0% is recommended to ensure construction safety.

2.3. Fracturing Method and Column Design. For the design of the fracturing method and the fracture column structure, the construction friction during the fracture process must be considered first. In fracture construction, frictional resistance affects construction pressure, which affects construction safety and success rate. Friction is related to the type of fracturing fluid, injection mode, displacement, and foam mass.

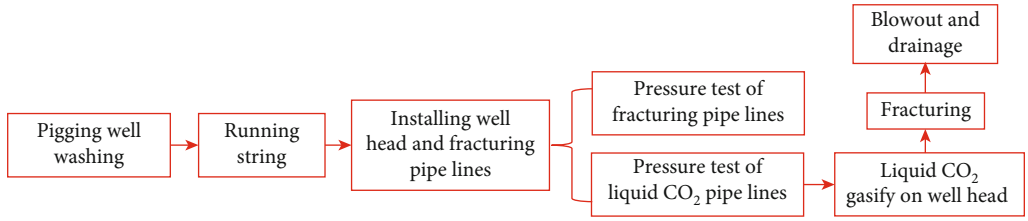

Figure 7: Operating technique process.

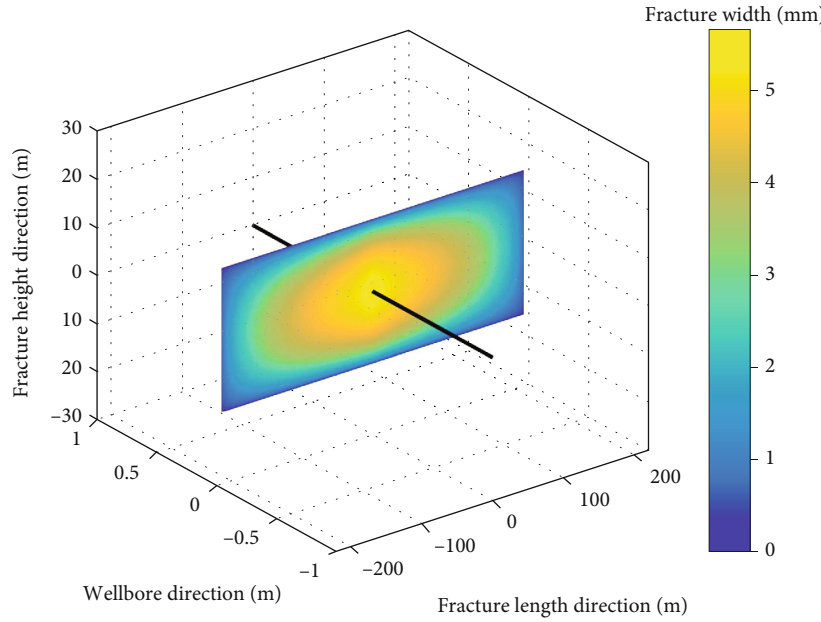

Figure 8: Fracture morphology of carbon dioxide foam fracturing (displacement 4.0 m^3/min).

While CO_2 foam fracturing, the CO_2 foam mass during pumping process should be firstly considered. The quality of the foam is robust, and the fracturing fluid system has a high viscosity and favorable sand-carrying properties. If the displacement of the pumped liquid CO_2 is large, it will be pumped into the formation without blistering, reducing the sand-carrying performance. Therefore, the use of a high-displacement chamber injection method is not recommended. Because CO_2 foam fracturing fluid itself has high frictional resistance, CO_2 foam fracturing adopts the tubing injection method, and 2 7/8″ and 3 1/2″ oil pipes are used to simulate the relationship between friction and flow of CO_2 foam fracturing. Figure 5 shows that under the same displacement, the frictional resistance injected by the 3 1/2″ tubing is much smaller than that of the 2 7/8″ tubing. From the perspective of reducing the friction of the fracturing column and ensuring construction safety, the column of CO_2 foam fracturing selects 3 1/2″ tubing.

The goal of shale reservoir fracturing conversion in the Sichuan Basin is to achieve large displacement and large-scale volumetric fracturing conversion effects. From the perspective of constructive displacement and liquid scale, CO_2 foam fracturing cannot achieve large displacements at this stage. Construction requirements, and thus volume transformation effects, are difficult to achieve.

3. Construction Procedure for CO_2 Foam Fracturing

The CO_2 foam fracturing construction process is divided into two main parts: the pumping procedure and the construction process.

3.1. Pumping Procedure. Pumping procedures include fracture fluid injection procedure and liquid CO_2 phase injection procedure. During the CO_2 foam fracturing construction, the proppant concentration (sand ratio) is inevitably reduced after the sand-carrying liquid is mixed with the liquid CO_2. To improve the construction sand ratio, the design concept of "constant internal phase" is adopted, that is, the internal phase (CO_2 gas+proppant) is balanced with the external phase (freeze fracturing fluid) to ensure the viscosity of the fracturing fluid is constant. When the proppant concentration is increased, the displacement of the base fluid of the jelly fracture fluid remains stable, and the displacement of the liquid CO_2 decreases correspondingly, with a decrease equal to the absolute displacement of the proppant. Although a constant internal phase can increase the sand ratio, the improvement is limited. In the later stages of construction, however, when the temperature of the fracturing fluid in the formation is very low and the fraction of the

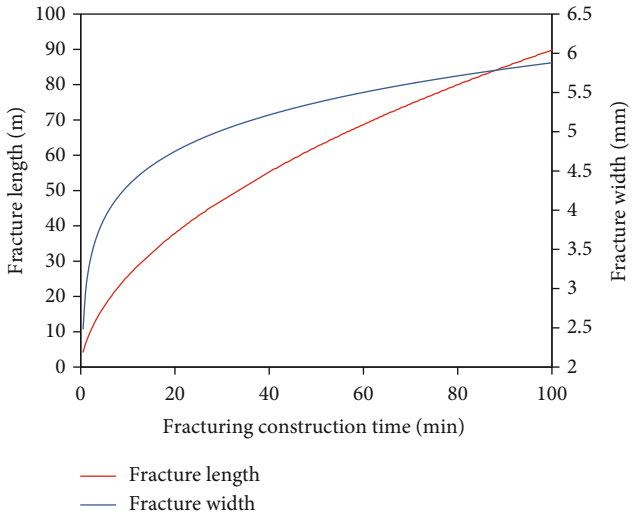

Figure 9: Fracture morphology of carbon dioxide foam fracturing (displacement 4.0 m^3/min).

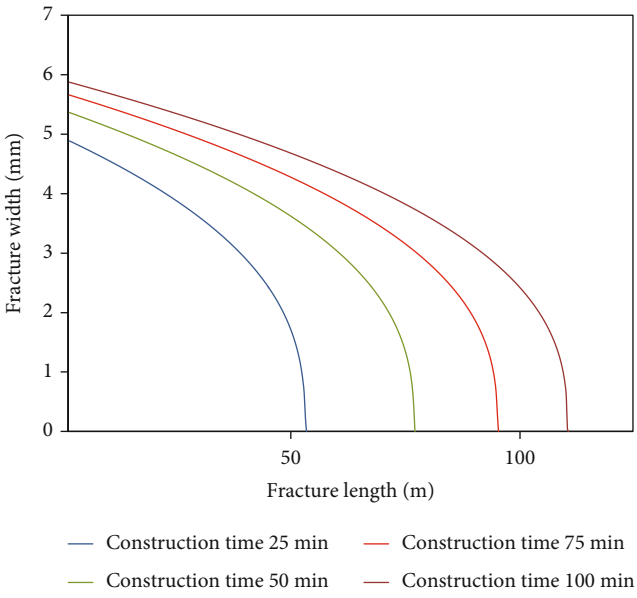

Figure 10: Fracture morphology of carbon dioxide foam fracturing under different construction times (displacement 4.0 m^3/min).

foam fracturing fluid is becoming smaller and smaller, it is necessary to make full use of the jelly fracturing fluid. The sand carrying capacity increases the sand ratio. Therefore, the design idea of "constant internal phase+variable foam quality" is adopted, that is, when the proppant concentration is increased, the displacement of the jelly fracturing fluid is kept stable, the foam quality is gradually changed, and the ratio of liquid CO_2 increases with the sand ratio. Gradually decreasing, to sufficiently utilize the sand carrying capacity of the Jell-O fracturing fluid during the high sand ratio phase, further increasing the sand ratio.

The initial CO_2 foam mass of the fracture design is 75%. The main reasons are as follows: (1) designing larger foam quality in the initial stage, which can increase formation energy and (2) reducing fracturing fluid loss and reducing water-sensitive reservoir damage. The half-life of the foam and the overall construction time are about 2-4 hours. When the foam mass is 75%, the viscosity of the fracturing fluid is the largest and the sand carries the best. As the construction progresses, the temperature of the fracturing fluid in the formation gradually decreases, the fraction of the foam fracturing fluid becomes smaller and smaller, and the foam mass becomes smaller and smaller. Therefore, it is necessary to make full use of the sand carrying capacity of the jelly fracturing fluid to improve the sand ratio.

3.2. Construction Process. In the process of CO_2 foam fracturing (Figures 6 and 7), the friction is high, so it is generally preferred to select a large-sized fracturing string (such as a 3 1/2″ oil pipe or an oil jacket annulus).

3.3. Construction Displacement. When the construction displacement is set to 4.0 m^3/min and the construction time is 100 min, the fracture geometry is obtained as shown in Figure 8. As can be seen from Figure 9, the fracture extension length of this model can reach about 100 m with a maximum width of 6 mm at the fracture center at the specified construction displacement and construction time. Throughout the fracture length direction, the fracture width gradually decreases. In terms of the trend, the trend of the fracture width is that the decreasing range from the mouth of the fracture to the tip gradually increases.

Figure 10 shows the variation of the fracture length and width within 100 min of construction. As the construction time continues to increase, the fracture length and width gradually increase, with the trend being that the increase is larger in the early stages of construction. This is because the construction time is short, the fracture extension distance is short, and the fracture wall area is small, so the filtration effect is small and more fluid is involved in the joint formation. However, as the construction time increases, the fracture extension distance becomes longer and the fracture wall area becomes larger, so the filtration effect is enhanced, the number of filtrates increases, and the fracture extension speed slows down, leading to a slow increase in fracture length and width.

4. Conclusions

(1) Combined with the goal and idea of shale reservoir fracturing in the Sichuan Basin, the pump design of CO_2 foam fracturing adopts "constant internal phase+variable foam quality," and the quality of construction foam is controlled at 52% ~75%

(2) Optimized the column and displacement design and simulated the CO_2 foam fracturing friction under different displacements of 2 7/8″ and 3 1/2″ tubing. The sand ratio was designed to be 18.0% to 22.0% according to the sedimentation theory of CO_2 foam fracturing fluids. Depending on liquid CO_2 storage, column structure, and scale characteristics, a total

construction displacement of $2.5 \sim 5.0\,m^3$/min is preferred

(3) The CO_2 foam fracturing pump injection procedure and the construction process procedure was established to provide a reference for testing the onsite process technology. The fracture morphology of CO_2 foam fracturing is simulated to obtain the fracture spreading behavior at different construction displacements and times, which can satisfy the fracture length achieved by conventional fracturing

Data Availability

The data used to support the findings of this study are available from the corresponding author upon request.

Conflicts of Interest

The authors declare that they have no conflicts of interest.

Authors' Contributions

Conceptualization and writing—review and editing were performed by C. Gao. Conceptualization and methodology were performed by S. Cheng. Methodology and software and resource acquisition were contributed by M. Wang. Validation and data curation were performed by W. Wu. Writing—review and editing was performed by S. Li. Project administration was performed by Z. Gao. Funding acquisition was performed by X. Meng. All authors have read and agreed to the published version of the manuscript.

Acknowledgments

This work was supported by the National Natural Science Foundation of China: Study on dynamic characteristics of methane/carbon dioxide in shale heterogeneous reservoir under multi-field coupling (Program No. 41772150).

References

[1] D. Dong, S. Gao, J. Huang, Q. Guan, S. Wang, and Y. Wang, "A discussion on the shale gas exploration & development prospect in the Sichuan Basin," *Natural Gas Industry*, vol. 2, no. 1, pp. 9–23, 2014.

[2] X. Qian and J. Zhang, "Exploration and development technology of shale oil and gas in the world: progress, impact, and implication," *IOP Conference Series: Earth and Environmental Science*, vol. 526, article 012131, 2020.

[3] C. Boyer, J. Kieschnick, R. Suarez-Rivera, R. E. Lewis, and G. Waters, "Producing gas from its source," *Oilfield Review*, vol. 18, no. 3, pp. 36–49, 2006.

[4] Z. H. Juntao, W. Jinqiao, G. Zhiliang, and D. Haomin, "Research and application of slick water fracturing fluid on continental shale reservoir," *Unconventional Oil & Gas*, vol. 1, no. 1, pp. 55–59, 2014.

[5] C. H. Pengfei, L. I. Youquan, D. E. Sufen et al., "Research and application of slick water for shale volume fracturing," *Chemical Engineering of Oil & Gas*, vol. 42, no. 3, pp. 270–273, 2013.

[6] Y. Q. Xia, "The challenges of water resources and the environmental impact of Marcellus shale gas drilling," *Science & Technology Review*, vol. 28, no. 18, pp. 103–110, 2010.

[7] X. R. Luo, S. Z. Wang, Z. F. Jing, and Z. G. Wang, "Experimental research on rheological properties of slick water mixed with CO_2 system," *Advanced Materials Research*, vol. 910, pp. 95–100, 2014.

[8] Y. Chen and T. L. Pope, "Novel CO_2-emulsified viscoelastic surfactant fracturing fluid system," in *SPE European Formation Damage Conference*, Scheveningen, The Netherlands, 2005.

[9] Z. Zhang, J. Mao, X. Yang, J. Zhao, and G. S. Smith, "Advances in waterless fracturing technologies for unconventional reservoirs," *Energy Sources, Part A: Recovery, Utilization, and Environmental Effects*, vol. 41, no. 2, pp. 237–251, 2019.

[10] L.-L. Wang, T.-F. Wang, J.-X. Wang, H.-T. Tian, Y. Chen, and W. Song, "Enhanced oil recovery mechanism and technical boundary of gel foam profile control system for heterogeneous reservoirs in Changqing," *Gels*, vol. 8, no. 6, p. 371, 2022.

[11] X. Sun, X. B. Liang, S. Z. Wang, and Y. Lu, "Experimental study on the rheology of CO_2 viscoelastic surfactant foam fracturing fluid," *Journal of Petroleum Science and Engineering*, vol. 119, pp. 104–111, 2014.

[12] A. S. Emrani, A. F. Ibrahim, and H. A. Nasr-El-Din, "Mobility control using nanoparticle-stabilized CO_2 foam as a hydraulic fracturing fluid," in *SPE Europec featured at 79th EAGE Conference and Exhibition*, Paris, France, 2017.

[13] A. S. Emrani and H. A. Nasr-El-Din, "Stabilizing CO_2 foam by use of nanoparticles," *SPE Journal*, vol. 22, no. 2, pp. 494–504, 2017.

[14] H. T. Zhu, D. L. Chen, H. J. Liu, and T. C. Zhou, "Application of carbon dioxide foam fracturing technology in low-permeability and tight gas reservoir of western Sichuan," *Drilling & Production Technology*, vol. 32, no. 1, pp. 53-54, 2009.

[15] M. J. Liu, "Pilot research of CO_2 foam fracturing in Daniudi low permeability gas field," *Inner Mongolia Petrochemical Industry*, vol. 17, pp. 108–110, 2008.

[16] X. M. Pan and W. G. Shen, "An attempt to stimulate low permeability oilfield by CO_2 fracturing," *Special Oil & Gas Reservoirs*, vol. 12, no. 6, pp. 85–87, 2005.

[17] M. M. Reynolds, R. C. Bachman, and W. E. Peters, "A comparison of the effectiveness of various fracture fluid systems used in multi-stage fractured horizontal wells: Montney formation, unconventional gas," in *SPE Hydraulic Fracturing Technology Conference*, The Woodlands, Texas, USA, 2014.

[18] D. V. S. Gupta, B. T. Hlidek, E. S. W. Hill, and H. S. Dinsa, "Fracturing fluid for low-permeability gas reservoirs: emulsion of carbon dioxide with aqueous methanol base fluid: chemistry and applications," in *SPE Hydraulic Fracturing Technology Conference*, College Station, Texas, USA, 2007.

[19] Z. D. Wang, X. Q. Wang, and Y. J. Lu, "Application of carbon dioxide foam fracturing technology in low-permeability and low-pressure gas reservoirs," *Acta Petrolei Sinica*, vol. 25, no. 3, pp. 66–70, 2004.

[20] C. L. Gong, *Theory and Technology Research of Carbon Dioxide Foamed Fracturing*, Southwest Petroleum University, Chengdu, 2009.

[21] X. Q. Zheng and Z. X. Jin, "*Optimizing design technology and application of CO_2 foam fracturing*," vol. 25, Tech. Rep. 4, Oil Drilling & Production Technology, 2013.

[22] Q. Wang and X. D. Wu, "Phase and physical property calculated model of gas, liquid, and supercritical CO_2," *Journal of*

the Shengli College China University of Petroleum, vol. 26, no. 2, pp. 11–14, 2012.

[23] R. L. Mazza, "Liquid-free CO_2/sand stimulations: an overlooked technology production update," in *SPE Eastern Regional Meeting*, Canton, Ohio, 2001.

[24] C. Xiao, S. N. Balasubramanian, and L. W. Clapp, "Rheology of supercritical CO_2 foam stabilized by nanoparticles," in *SPE Improved Oil Recovery Conference*, Tulsa, Oklahoma, USA, 2016.

[25] L. Wang, B. Yao, M. Cha et al., "Waterless fracturing technologies for unconventional reservoirs-opportunities for liquid nitrogen," *Journal of Natural Gas Science and Engineering*, vol. 35, pp. 160–174, 2016.

[26] N. B. Alqatahni, M. Cha, B. Yao et al., "Experimental investigation of cryogenic fracturing of rock specimens under true triaxial confining stresses," in *SPE Europec featured at 78th EAGE Conference and Exhibition*, Vienna, Austria, 2016.

[27] S. R. Grundmann, G. D. Rodvelt, G. A. Dials, and R. E. Allen, "Cryogenic nitrogen as a hydraulic fracturing fluid in the Devonian shale," in *SPE Eastern Regional Meeting*, Pittsburgh, Pennsylvania, 1998.

[28] L. Jiang, Y. Cheng, Z. Han et al., "Effect of liquid nitrogen cooling on the permeability and mechanical characteristics of anisotropic shale," *Journal of Petroleum Exploration and Production Technology*, vol. 9, pp. 111–124, 2018.

[29] C. K. Fu and N. Liu, "Waterless fluids in hydraulic fracturing - A review," *Journal of Natural Gas Science and Engineering*, vol. 67, pp. 214–224, 2019.

[30] F. Shen, H. Yang, T. Liu, B. Lin, G. J. Chen, and K. Tan, "Application of high-temperature clean CO_2 foam fracturing fluid in shale gas reservoirs," *Oil Drilling & Production Technology*, vol. 38, no. 1, pp. 93–97, 2016.

[31] P. Tan, H. Pang, R. Zhang et al., "Experimental investigation into hydraulic fracture geometry and proppant migration characteristics for southeastern Sichuan deep shale reservoirs," *Journal of Petroleum Science and Engineering*, vol. 184, article 106517, 2020.

[32] P. Tan, Y. Jin, and H. W. Pang, "Hydraulic fracture vertical propagation behavior in transversely isotropic layered shale formation with transition zone using XFEM-based CZM method," *Engineering Fracture Mechanics*, vol. 248, article 107707, 2021.

[33] C. Fu and N. Liu, "Rheology and stability of nanoparticle-stabilized CO_2 foam under reservoir conditions," *Journal of Petroleum Science and Engineering*, vol. 196, article 107671, 2021.

[34] M. Wang, W. Wu, S. Chen et al., "Experimental evaluation of the rheological properties and influencing factors of gel fracturing fluid mixed with CO_2 for shale gas reservoir stimulation," *Gels*, vol. 8, no. 9, p. 527, 2022.

[35] C. Cai, B. R. Li, Y. Y. Zhang et al., "Fracture propagation and induced strain response during supercritical CO_2 jet fracturing," *Petroleum Science*, vol. 19, no. 4, pp. 1682–1699, 2022.

[36] Z. Cong, Y. Li, Y. Pan et al., "Study on CO_2 foam fracturing model and fracture propagation simulation," *Energy*, vol. 238, article 121778, 2022.

[37] W. A. M. Wanniarachchi, P. G. Ranjith, M. S. A. Perera, A. Lashin, N. Al Arifi, and J. C. Li, "Current opinions on foam-based hydro-fracturing in deep geological reservoirs," *Geomechanics and Geophysics for Geo-Energy and Geo-Resources*, vol. 1, no. 3-4, pp. 121–134, 2015.

[38] N. Yekeen, E. Padmanabhan, and A. K. Idris, "A review of recent advances in foam-based fracturing fluid application in unconventional reservoirs," *Journal of Industrial and Engineering Chemistry*, vol. 66, pp. 45–71, 2018.

[39] X. Luo, X. Ren, S. Wang, X. Li, H. Ma, and Y. Liu, "Experimental study on convection heat-transfer characteristics of BCG-CO_2 fracturing fluid," *Journal of Petroleum Science and Engineering*, vol. 160, pp. 258–266, 2018.

[40] G. Dazhi and R. I. Tanner, "The drag on a sphere in a power-law fluid," *Journal of Non-Newtonian Fluid Mechanics*, vol. 17, no. 1, pp. 1–12, 1985.

[41] V. A. Kuuskraa, J. P. Brashear, L. E. Elkins, and F. Morra, "Gas recovery from tight formations is a function of technology and economics," *Journal of Petroleum Technology*, vol. 33, no. 8, pp. 1545–1556, 1981.

[42] G. Nolte, A. Ziehe, N. Krämer, F. Popescu, and K.-R. Müller, "Comparison of granger causality and phase slope index," in *Proceedings of Workshop on Causality: Objectives and Assessment at NIPS 2008*, pp. 267–276, Vancouver, British Columbia, Canada, 2010.